Comparing Different Approaches for Moisture Transfer inside Constructions with Air Gaps

L. Nespoli[1], M. Bianchi Janetti[*2], and F. Ochs[2]

[1]Politecnico di Milano, Dipartimento di Energetica, Milano, Italy,
[2]University of Innsbruck, Unit for Energy efficient Buildings, Innsbruck, Austria
*Corresponding author: Technikerstr. 13, A-6020 Innsbruck, email: michele.janetti@uibk.ac.at

Abstract: A model for the conjugate simulation of heat and moisture transfer inside porous materials and fluid domains is implemented in Comsol. The results of this model are compared with those obtained through a simplified approach: the line-source approach.

The models are both validated with experimental data and with numerical results from other authors.

On the one hand the conjugate approach is able to predict better results from a physical point of view, since it calculates the velocity field inside the air cavities through computational fluid dynamics (CFD); on the other hand, including fluid dynamics in long period hygrotermal simulation increases numerical effort and computational time. Thus the simplified approach can be advantageous e.g. in building physics applications presenting complex geometry and long simulation time.

Keywords: Heat and Moisture Transfer, CFD, Building Physics.

1. Introduction

In recent times the use of numerical simulation for predicting heat and moisture transfer inside construction is increasing.

In external walls with embedded timber beams, the analysis of the moisture risk is of paramount importance, since water condensation can lead to structural damage. If an internal insulation is applied (e.g. in case of historical buildings for which an external insulation is not always possible) the risk of structural damage could arise [1]. Moreover, the presence of air gaps can significantly influence the moisture distribution. In such a situation a high quality energy retrofit must be studied, in order to guarantee a long term preservation of the building. Many studies on this topic including numerical analysis and in-situ measurements have been published [2],[3].

Numerical simulation can supply important information for a correct design and for the choice of proper materials. At present, specific software for hygrothermal simulation in building-physics application, based on the works of Künzel [4] and Grunewald [5], are available [6], [7]. This software enables HAM (Heat, Air, Moisture) modeling in porous media; however CFD is not yet included. A study concerning conjugate HAM-CFD modeling and benchmark experiments has been recently performed by van Belleghem [8], however his model is valid only in the hygroscopic range (RH<98%).

The use of Comsol can be profitable for HAM and CFD modeling. Some building-physics applications in this field have been already realized by van Schijndel [9]. Comsol has been tested also in capillary-moisture range (RH>98%); however for moisture values close to the saturation numerical instability can occur in some cases [10], [11].

In this study a conjugate model for heat and moisture transfer in construction including CFD in fluid domains is developed,.

Since this realistic modeling may present high complexity and significant computational effort also a simplified approach, convenient for long-period simulation, is derived.

In the first part of the paper the mathematical model is described. In the second part both the approaches are applied on two exemplary cases.

2. Governing Equations and use of COMSOL Multiphysics

2.1. Heat and moisture transfer in porous domains

The heat and moisture transfer processes in the porous domains can be described by a system of two partial differential equations derived by imposing the equilibrium balance of mass and energy within an infinitesimal element of volume. Following the governing equations are reported:

$$\frac{\partial u}{\partial \varphi}\frac{\partial \varphi}{\partial t} + \nabla \cdot \left(-D_{m,\varphi}\nabla\varphi - D_{m,T}\nabla T\right) = 0 \tag{1}$$

$$\frac{\partial h}{\partial T}\frac{\partial T}{\partial t} + \frac{\partial h}{\partial \varphi}\frac{\partial \varphi}{\partial t} + \nabla \cdot \left(-D_{e,T}\nabla T - D_{e,\varphi}\nabla\varphi\right) = 0 \tag{2}$$

Temperature T and relative humidity φ are the dependent variables whereas t and x represent time and position. u is the moisture content and h the enthalpy. $D_{m,\varphi}$, $D_{m,T}$, $D_{e,T}$ and $D_{e,\varphi}$ are material specific functions depending from T and φ. The derivation of these material functions can be found in [4], [5], [12] and is not repeated. Equations (1) and (2) are introduced in Comsol Multiphysics selecting in the Model Navigator: PDE Modes → PDE, Coefficient Form → Time-dependent analysis. The equation coefficients are assigned in the Subdomain Setting-Window of the Comsol Multiphysics GUI.

Notice that the PDE system (1) and (2) leads to a mass conservation error if implemented in Comsol [13], however this error is acceptable if adequate numerical measures are employed [10], [11].

2.1. Heat and moisture transfer in fluid domains (conjugate approach)

In the conjugate approach, both the porous material domain and the fluid domain (air) are solved within the same solver. In this way there is no need for transfer coefficients to couple heat and mass transfer between both domains.

The following balance equations are employed:

$$F\frac{\partial \varphi}{\partial t} + \nabla \cdot \left(-D_{m,\varphi,a}\nabla\varphi - D_{m,T,a}\nabla T\right) \\ + \varphi\left(\frac{\partial F}{\partial t} + \boldsymbol{v}\nabla F\right) + F\boldsymbol{v}\nabla\varphi \\ = 0 \tag{3}$$

$$A_T\frac{\partial T}{\partial t} + A_\varphi\frac{\partial \varphi}{\partial t} + \nabla \cdot \left(-D_{e,T,a}\nabla T - D_{e,\varphi,a}\nabla\varphi\right) \\ - \boldsymbol{v}\left(A_\varphi\nabla\varphi + A_T\nabla T\right) = 0 \tag{4}$$

with:

$$F = \frac{p_s}{R_v T} \tag{5}$$

$$D_{m,\varphi,a} = D_v F \tag{6}$$

$$D_{m,T,a} = D_v\varphi\frac{\partial F}{\partial T} \tag{7}$$

$$D_{e,\varphi,a} = D_v\left(h_v^* - h_{a,d}^*\right)F \tag{8}$$

$$D_{e,T,a} = D_v\left(h_v^* - h_{a,d}^*\right)\varphi\frac{\partial F}{\partial T} + \lambda_a \tag{9}$$

$$A_\varphi = \left(h_v^* - h_{a,d}^*\right)F \tag{10}$$

$$A_T = \left(h_v^* - h_{a,d}^*\right)\varphi\frac{\partial F}{\partial T} + \varphi F\left(c_v - c_{a,d}\right) \\ + \rho_{a,d}c_{a,d} \tag{11}$$

Equation (3) and (4) are obtained according to [14] but neglecting the gravitational acceleration. The derivation of eq. (6)-(11) can be found in [15].

2.2. Momentum and continuity equations in fluid domains (conjugate approach)

The velocity field inside the fluid domains is calculated with the CFD module of Comsol. The incompressible Navier-Stokes equation and the continuity equation are employed:

$$\rho\frac{\partial \boldsymbol{v}}{\partial t} + \rho\boldsymbol{v} \cdot \nabla\boldsymbol{v} = \nabla \cdot \left(-p\boldsymbol{I} + \boldsymbol{\tau}\right) \tag{12}$$

$$\frac{\partial \rho}{\partial t} = -\nabla \cdot (\rho\boldsymbol{v}) \tag{13}$$

Where p and $\boldsymbol{\tau}$ are the total pressure and the viscous stress tensor respectively. ρ is the air density and $\boldsymbol{I}$ is the identity matrix. Assuming a Newtonian fluid, together with Stokes assumption and incompressibility, the viscous stress tensor can be written as:

$$\boldsymbol{\tau} = 2\mu\boldsymbol{S} \tag{14}$$

Where μ is the dynamic viscosity and $\boldsymbol{S}$ is the strain-rate tensor, defined as the symmetric part of the velocity gradient:

$$\boldsymbol{S} = \frac{1}{2}\left(\nabla\boldsymbol{v} + (\nabla\boldsymbol{v})^T\right) \tag{15}$$

2.3 Line-source equations

Applying the simplified line-source approach according to [16], the forced convection of moisture and energy inside a thin air gap is described by the following balance equations:

$$A\left(\frac{\partial \rho_v}{\partial t} + v\frac{\partial \rho_v}{\partial s}\right) = L\beta_k(p_{v,b} - p_{v,a}) \tag{16}$$

$$A\left(\frac{\partial h_a}{\partial t} + v\frac{\partial h_a}{\partial s}\right) = L[\alpha_k(T_b - T_a) \tag{17}$$
$$+ \beta_k(p_{v,b} - p_{v,a})h_v]$$

where s and t represent the position along the gap axis and the time. ρ_v and p_v are the water vapor density and the partial pressure of water vapor in the air. h_a and T_a are the specific enthalpy of the air and the air temperature. T_b and $p_{v,b}$ are the temperature and the partial pressure of the water vapor on the boundary of the air gap. β_k and α_k are the convective transfer coefficients for moisture and energy at the gap surfaces. v represent the bulk air velocity, which is supposed to be directed along the gap axis, A is the gap cross-section area and L is the length of the cross-section perimeter.

The partial pressure of water vapor depends on the temperature and the water vapor density through the ideal gas equation ($p_v = \rho_v R_v T$).

The specific enthalpy of humid air is described by the following equation:

$$h_a = \rho_{a,d}c_{p,a,d}T + \rho_v(h_{lv} + c_{p,v}T) \tag{18}$$

where the term $\rho_{a,d} \cdot h_{a,d} \cdot T$ represents the enthalpy of dry air, whereas $\rho_v \cdot (h_{lv} + c_{p,v} \cdot T)$ represents the enthalpy of water vapour.

3. Results

3.1 Test case A: comparison with experimental data

In order to validate the implemented models, results calculated with the conjugate approach and with the line-source approach are compared with measured data from the literature and with numerical results by other authors.

The test-bed described in [17] is modeled in COMSOL (see Figure 1). Three overlapped gypsum boars (each 12,5cm thick) are firstly humidified and then dried by steaming air inside a duct (forced convection, fully developed laminar flow). Measured values of temperature and relative humidity are available at different positions between the gypsum boards. Detailed information concerning the position of the sensors and the material properties can be found in [17].

Consider that the results by the other authors are obtained employing one-dimensional simulations. This is justified, as in this specific case temperature and moisture vary significantly only along the depth of the gypsum (y axis). Both the line source and the conjugate approaches are more generally applicable, since they consider also variations in the other direction (along the x axis).

In Figure 2 the time evolution of relative humidity and temperature are reported.
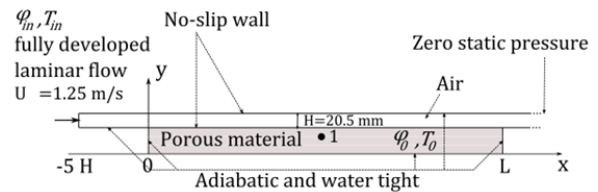
Figure 1. Geometry and boundary condition for the test case A
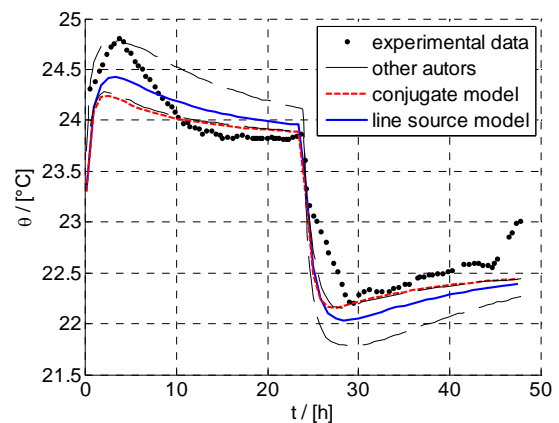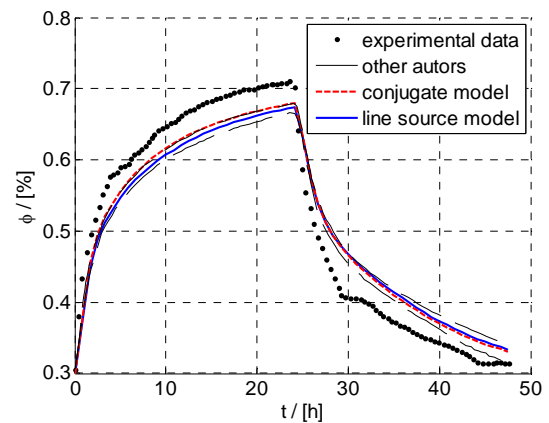
Figure 2. Time evolution of relative humidity (top) and temperature (bottom) at x=0.5m and at a depth of 12.5mm (point 1 in Figure 1).

Minor deviations concerning the relative humidity are present between the various numerical results. Also the deviation in the temperature development is acceptable, considering that the absolute variation of temperature is rather small.

Significant deviations are present between simulated and measured values, in particular for the relative humidity evolution. This is explained in [17] considering the uncertainties on the material data.

3.1 Test case B

In the previous test (case A) no significant difference between the line-source and the conjugate model has been assessed. This can be justified considering that the flow is fully developed and the transfer coefficients remain almost constant along the channel axis. In case of no fully-developed flow a larger discrepancy between the two models is expected.

In this section we consider a gypsum component exchanging heat and moisture with air streaming inside a bended channel (see Figure 3).

Constant convective coefficients for heat transfer (α_k=46.2 W/(m^{2}K)) and for the vapour transfer (β_k=3e-7 s/m) are employed in the line-source model according to [16]. Detailed information regarding the model set-up are available in [15]. In this case no experimental data are available.

At the channel corner the flow generate a vortex; therefore we expect a discrepancy between the two models downstream of this position.

In Figure 4 the distribution of relative humidity and temperature calculated with the conjugate model are reported after one hour.

In Figure 5 the relative deviation between the two employed approaches is shown for both relative humidity and temperature.

The maximal relative deviation for φ and T is reached at the corner (point 2 in Figure 3) at the outlet (point 1) respectively.

In Figure 6 the time development of the relative deviations at these two points is reported. The relative deviations are calculated using the following formula:

$$u_{deviation} = \frac{u_c - u_{ls}}{u_c} \tag{19}$$

Where u_c and u_{ls} represent the solutions from the conjugate and from the line-source approach respectively. The simulation time results significantly lower for the line-source approach (see Table 1). These results are obtained with a processor Intel Core i3 350M a 2.27 GHz, RAM 4GB.
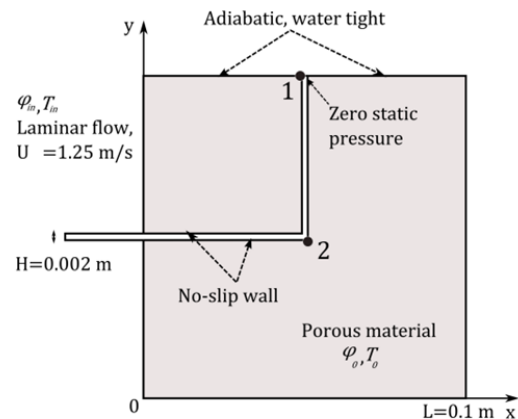

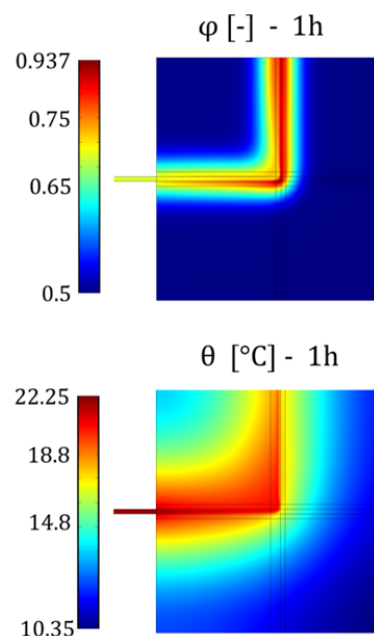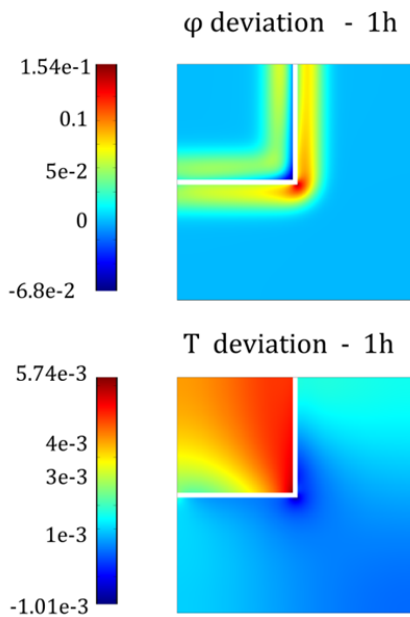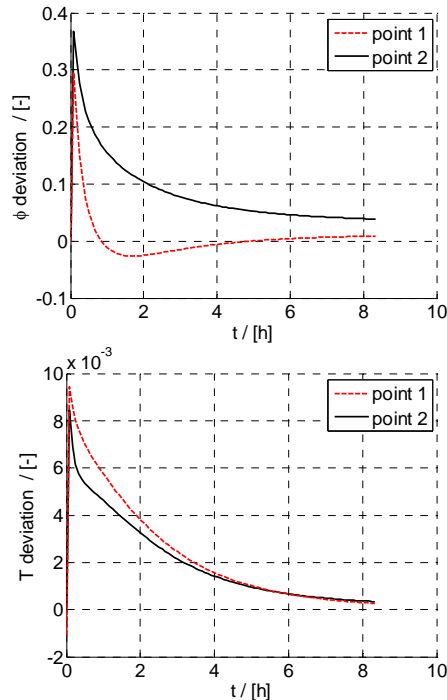**Figure 3.** Geometry and boundary condition for the test case B

Figure 4. Values of relative humidity [-] (top) and temperature [K] (bottom) for the conjugate approach after 1h.

Figure 5. Relative differences between the conjugate and the line source approach, for relative humidity (top) and temperature (bottom) after 1h.

Figure 6. Time evolution of the relative error for temperature and relative humidity at point 1 and 2 (see Figure 3)

Table 1 Simulation time and degrees of freedom

Approach	Sim. Time [s]	D.O.F
Line-source	45	13444
Conjugate	156	23256

4. Conclusion and outlook

The line-source approach can be advantageous since the numerical effort is reduced comparing with the conjugate approach. However, the deviation between the two approaches becomes important just near the vortex.

The results presented in this paper concern forced convection in laminar flow. Further work on the modeling of free convection and turbulent flow in air cavities will be performed.

Conservative modeling and realistic driving rain simulation using Comsol are not yet adequately investigated.

5. Acknowledgements

6. Nomenclature

A	$[m^2]$	Cross-section area
A_φ	$[J/m^3]$	Energy storage term
A_T	$[J/m^3K]$	Energy storage term
c	$[J/(kg\ K)]$	Heat capacity
D	$[m^2/s]$	Diffusivity
Dm,φ	$[kg/(m\ s)]$	
Dm,T	$[kg/(m\ s\ K)]$	Transport
De,φ	$[W/m]$	coefficients
De,T	$[W/(m\ K)]$	
F	$[Kg/m^3]$	Moisture storage term
h^*	$[J/Kg]$	Specific enthalpy
h	$[J/m^3]$	Volumetric enthalpy
L	$[m]$	Cross-section perimeter
p	$[Pa]$	Pressure
q	$[W/m]$	Heat source
R	$[J/(kg\ K)]$	Gas constant
t	$[s]$	Time
T	$[K]$	Temperature

θ	$[°C]$	Temperature
u	$[kg/m^3]$	Volumetric water content
v	$[m/s]$	Velocity
α	$[W/(m^2 K)]$	Heat transfer coefficient
β	$[s/m]$	Mass transfer coefficient
λ	$[W/m\ K]$	Thermal conductivity
ρ	$[kg/m^3]$	Density
φ	$[\%]$	Relative humidity
τ		Stress tensor

Subscripts

a	Air
b	Boundary
d	Dry
k	Convective
l	Liquid
p	Constant pressure
v	Vapor
s	Saturation

6. References

[1] R. Pfluger, "Lösungen für den Feuchteschutz. Protokollband Nr.32. Fektor 4 auch bei sensiblen Altbauten: Passivhauskomponeneten + Innendämmung. Darmstadt," 2005.

[2] U. Ruisinger, "Long-term measurements and simulations of five internal insulation systems and their impact on wooden beam heads," *CESBP Vienna*, pp. 313–319, 2013.

[3] D. Kehl, U. Ruisinger, R. Plagge, and J. Grunewald, "Wooden beam ends in masonry with interior insulation - A literature rewiew and simulation on causes and assessment of decay," *CESBP Vienna*, pp. 299–304, 2013.

[4] Künzel, "Simultaneous Heat and Moisture Transport in Building Components," *PhD, Fraunhofer Inst. Build. Phys.*, vol. 1995, 1995.

[5] J. Grunewald, "Diffusiver und konvektiver Stoff- und Energietransport in kapillarporösen Baustoffen," *Diss. Tech. Univ. Dresden*, 1997.

[6] "WUFi Software." http://www.wufi.de/, 2011.

[7] "Delphin Software." http://www.bauklimatik-dresden.de/delphin/, 2011.

[8] M. Van Belleghem, M. Steeman, a. Willockx, a. Janssens, and M. De Paepe, "Benchmark experiments for moisture transfer modelling in air and porous materials," *Build. Environ.*, vol. 46, no. 4, pp. 884–898, Apr. 2011.

[9] A. W. M. van Schijndel, "Integrated Heat Air and Moisture Modeling and Simulation," *PhD Diss. Eindhoven, Univ. Technol.*, 2007.

[10] M. Bianchi Janetti, F. Ochs, and W. Feist, "On the conservation of mass and energy in hygrothermal numerical simulation with COMSOL Multiphysics," *Build. Simul. Conf. Chambery*, 2013.

[11] M. B. Janetti, F. Ochs, and W. Feist, "Numerical Quality of a Model for Coupled Heat and Moisture Transport in COMSOL Multiphysics," 2012.

[12] M. Bianchi Janetti, F. Ochs, and W. Feist, "3D Simulation of Heat and Moisture Diffusion in Constructions," *Comsol Conf. Stuttgart 2011*, 2011.

[13] H. Janssen, B. Blocken, and J. Carmeliet, "Conservative modelling of the moisture and heat transfer in building components under atmospheric excitation," *Int. J. Heat Mass Transf.*, vol. 50, no. 5–6, pp. 1128–1140, Mar. 2007.

[14] T. Defraeye, B. Blocken, and J. Carmeliet, "Analysis of convective heat and mass transfer coefficients for convective drying of a porous flat plate by conjugate modelling," *Int. J. Heat Mass Transf.*, vol. 55, no. 1–3, pp. 112–124, Sep. 2011.

[15] L. Nespoli, "Analysis of heat and moisture transfer by conjugate modeling in building components (ongoing master thesis)," Politecnico di Milano, 2013.

[16] M. Bianchi Janetti, F. Ochs, and R. Pfluger, "Coupling Forced Convection in Air Gaps with Heat and Moisture Transfer inside Constructions," *Comsol Conf. Milano 2012*, 2012.

[17] C. James, C. J. Simonson, P. Talukdar, and S. Roels, "Numerical and experimental data set for benchmarking hygroscopic buffering models," *Int. J. Heat Mass Transf.*, vol. 53, no. 19–20, pp. 3638–3654, Sep. 2010.